KARYA ILHAM PUBLISHING
CONNECTING MINDS, BRIDGING IDEAS, INSPIRING READERS

International Communication in Computational Mechanics

Journal homepage:
https://karyailham.com.my/index.php/iccm
ISSN: 3093-7205

Improved Thermal Efficiency of Cooling of Offshore Wind Turbine Generators using Phase Change (PCM): CFD-Based Comparative Study

Moh Anton Rahmawijaya[1], Moch. Septian Dwi Rohmat Ari Wibowo[1], Muhammad Alfarid Zidan[1], Noval Isa Mahendra[1], Nikmah Izzatul Mukarromah[1], Sofi Patricia Putri[1], Misbahul Munir[1,*], Singgih Dwi Prasetyo[1]

[1] Power Plant Engineering Technology, Faculty of Vocational Studies, State University of Malang, Malang 65145, Indonesia

ARTICLE INFO

Article history:
Received 7 October 2025
Received in revised form 30 October 2025
Accepted 2 November 2025
Available online 4 November 2025

Keywords:

Cooling generators; offshore wind turbines; PCM; CFD; transient heat transfer; enthalpy–porosity; thermal efficiency

ABSTRACT

The maintenance and reliability of offshore wind turbine generators are impacted by heat accumulation in the corrosive and difficult-to-access marine environment, while conventional cooling often fails to withstand temperature surges and the creation of hot spots. This paper aims to determine the optimal PCM type, encapsulation design, and integration position. It also evaluates the extent to which PCM incorporation improves the thermal efficiency of an offshore generator cooling system. An enthalpy-porosity model was used in transient Computational Fluid Dynamics (CFD) simulations of the solid-liquid phase change material (PCM). At 50–100% load under forced and natural convection settings, three distinct PCM kinds (paraffin, hydrate salts, and eutectic mixes) as well as modifications to the encapsulation's placement and shape surrounding the stator coils and housing walls were investigated. PCM integration reduced the generator's peak temperature by 15–25% when compared to the reference without PCM; hydrate salts provided the best thermal homogeneity and the largest Tmax reduction (~22–25%); eutectic mixtures showed a balance between latent capacity and transient response (~20–23%); and paraffin offered the best cyclic stability despite a slower melting rate (~18–20%). Adjusted melting point, latent heat capacity, interfacial conductivity, and encapsulation design and location all affect final efficacy; prior to practical deployment, it is advised to improve heat transmission using conductive fillers or packed-bed structures.

1. Introduction

The development of offshore wind energy is increasingly important as a clean energy alternative to replacing fossil-fueled power plants. Because offshore wind turbines have more wind speed and stability than onshore turbines, they produce more electricity. But the engineering aspect presents a problem, particularly with regard to the longevity and dependability of electrical components. Generators are the key parts that are challenging to reach during maintenance and must function with high heat loads in humid and corrosive marine settings [1,2]. The performance, dependability,

* *Corresponding author.*
E-mail address: singgih.prasetyo.fv@um.ac.id

https://doi.org/10.37934/iccm.3.1.119

and component longevity of generators are all impacted by their cooling efficiency. When load fluctuations occur, conventional cooling systems are limited in their ability to maintain temperature stability. Excessive heat buildup can result in hot spots, harm insulation, reduce efficiency, and harm the generator. It highlights the necessity of creative cooling techniques that don't increase complexity or maintenance requirements [3,4].

Because they can both absorb and release thermal energy during phase transitions, phase change materials (PCMs) may be a solution. PCMs lower the thermal cycle, postpone the rise in excess temperature, and maintain the temperature at their melting point. PCM can enhance temperature dispersion, reduce temperature spikes, and increase cooling efficiency when used in the cooling of offshore wind turbine generators [5]. PCM has been successfully employed in earlier studies for heat control in batteries, solar systems, and electrical devices. Nevertheless, there are currently few research on the use of PCM in offshore wind turbine generator cooling systems. Additionally, the majority of previous research has not examined PCM kinds, capsulation shape, and integration techniques under conditions similar to those found in marine environments. Heat transfer can be effectively analyzed using numerical simulation techniques like Computational Fluid Dynamics (CFD), although comprehensive comparative studies are relatively uncommon [6,7].

1.1 Comparation of Article

Table 1
State of the art

References	Research focus	Key results
[8]	PCM for thermal management of electronic and rotating devices.	Effective for transient load cooling, but no CFD analysis on offshore wind turbine generators.
[9]	Experimental PCM cooling for PV modules under free and forced convection.	PCM reduced surface temperature by 20%; study limited to PV systems, not generator applications.
[10]	PCM-integrated cooling system using metal foam fins for transient thermal management.	Demonstrated transient CFD simulation improving heat transfer by 25%; DOI: 10.1016/j.ijheatmasstransfer.2023.124263.

These studies demonstrate at Table 1, the growing interest in phase change materials (PCM) as passive cooling media for electrical and renewable energy systems. Prior research successfully applied PCM to photovoltaic panels, electric vehicles, and electronic components, revealing notable temperature reductions and improved system reliability. However, despite significant progress, the application of PCM in offshore wind turbine generators remains underexplored. are taken from previous studies [1-10] focus on static or terrestrial systems such as PV modules, batteries, or EV motors, with limited consideration of the harsh marine environment characterized by high humidity, salinity, and unstable convection. Furthermore, few works provide a comparative CFD-based assessment of multiple PCM materials and encapsulation designs under dynamic load variations, which are critical to offshore generator performance.

Another limitation lies in the absence of transient modeling—many previous works rely on steady-state or simplified analytical formulations, which fail to capture the real-time thermal behavior of PCM melting and solidification. Similarly, geometry optimization and integration placement around high-heat components (such as stator windings and housing) are rarely investigated. This restricts practical guidance for offshore system designers seeking efficient, low-maintenance cooling alternatives.

1.2 Research Novelty

This research offers an original contribution by combining transient numerical simulations based on CFD (using the enthalpy-porosity formulation) with multi-material and multi-geometry comparative studies of PCM encapsulation in the context of *offshore wind turbine generators*—an application that has been rarely or not extensively studied in the PCM literature, which generally focuses on PV panels, small-scale TEGs, or land-based electronic components. By simulating real operating conditions in a coastal environment (ambient temperature range and convection coefficient variations reflecting natural and forced convection by sea breezes) as well as varying generator workloads (50–100% load), this study is able to more realistically represent the dynamics of PCM melting and freezing and its interaction with airflow and the generator's internal heat source than previous steady-state studies or 1-D models.

Methodologically, the novelty lies in the comprehensive approach that compares three types of PCM (paraffin, hydrated salts, and eutectic mixtures) simultaneously while evaluating several encapsulation designs (spherical, rectangular, cylindrical/packed-bed) and integration positions on the critical heat flow path (around the stator windings and housing wall). This combination provides a practical trade-off between latent capacity, transient response, and cyclic stability—information that is crucial for field implementation but rarely presented in an integrated manner in previous studies. Additionally, the research presents comprehensive quantitative metrics—peak temperature reduction, time delay to reach critical temperature, temperature homogeneity (CV), latent heat storage efficiency, and cyclic stability—allowing the results to be directly translated into technical design recommendations.

The practical implications of these findings also add to their novelty: not only do they show that PCM reduces Tmax (15–25%), but they also provide technical guidance in the form of material selection, encapsulation design, and heat transfer enhancement strategies (e.g., using conductive fillers or packed-bed structures) needed to bridge the gap between laboratory simulations and industrial deployment in a marine environment. Thus, this research is one of the first studies to systematically examine and formalize the use of PCM as a thermal management solution for offshore wind turbine generators, while also mapping critical issues (supercooling, cyclic degradation, the need for field testing) for further research.

2. Methodology
2.1 Research Design

This study examines the cooling system performance of offshore wind turbine generators using numerical simulations based on Computational Fluid Dynamics (CFD) [11]. Because of their thorough depiction of heat transport events, such as conduction, convection, and phase transition in phase change materials (PCM), CFDs were selected. Without conducting actual experiments in challenging maritime conditions, these simulations make it possible to assess the thermal behavior of cooling systems. The performance of cooling systems using PCM and traditional cooling systems was compared as part of the research technique. The type of PCM material (paraffin, salt hydrate, eutectic mixture), changes in capsulation geometry, and the location of PCM integration in heat flow are among the variables examined to determine the efficacy of PCM. Temperature distribution, peak temperature drop, and PCM's capacity to postpone crucial temperature rises are used to assess each simulation scenario. With this design, the research is expected to provide a deeper understanding of the influence of PCM design on the thermal efficiency of generator cooling systems. The results of the configuration comparison will be the basis for determining the optimal cooling strategy for offshore wind turbine operations. The study also seeks to develop practical design recommendations for wind turbine-based renewable energy technologies, to improve reliability, reduce the risk of thermal damage, and extend the life of generator components [8,12].

2.2 Geometry Models and Simulation Domains

In this study, the generator geometry model was simplified to balance the complexity of the calculation and the accuracy of the simulation. Simplification maintains the main heat transfer characteristics to keep the dominant thermal phenomenon accurate. This approach is important because overly detailed CFD simulations require large computational time, while overly simplistic representations can eliminate important physical mechanisms. Rotors and stators, which are heat sources for the conversion of electromagnetic energy, are the primary components that are modeled. The rotor generates heat from the friction losses and eddy currents, while the stator heats up due to the losses of the copper and core. The generator casing is also modeled as a conduction and convection medium to distribute heat to the surrounding environment. Thus, the heat flow from the source to the outer surface of the generator can be comprehensively analyzed. To evaluate the impact of geometry on latent heat absorption, Phase Change Material (PCM) units are introduced to geometric models in different capsulation shapes, including spherical, rectangular, and cylindrical packed beds. The contact surface area, melting speed, and heat distribution are taken into consideration while choosing the capsulation shape. Since the stator windings and housing walls have the maximum heat accumulation, the PCM is placed in the critical heat flow path around them. This setup makes it possible to assess how well the PCM distributes heat in the generator cooling system, delays peak temperature increases, and lessens temperature variations.

The internal parts of the generator, which include the rotor, shaft, bearing, spacer, and casing, are arranged in an exploded view in Figure 1**.** While maintaining the essential elements of heat transport, this image supports the geometric simplification strategy employed in the simulation. Heat sources (rotors and stators), conduction and convection mediums (casing), and heat flow pathways that are the subject of thermal analysis are represented by the components in the illustration [13]. This graphic serves as a spatial reference for the area with the greatest heat accumulation in CFD simulations, especially in the vicinity of the rotor and housing walls. Phase Change Material (PCM) units, which are modeled in several capsulation forms like cylindrical, rectangular, and spherical packed beds, are strategically placed in this area. To maximize latent heat absorption, reduce peak temperature rise, and enhance overall thermal distribution, the PCM form and position can be changed in relation to the image's physical configuration. In addition to supporting the accuracy of the geometric model employed, this picture offers crucial visual context for describing heat transfer fluxes and PCM-based cooling techniques in generator systems [14].

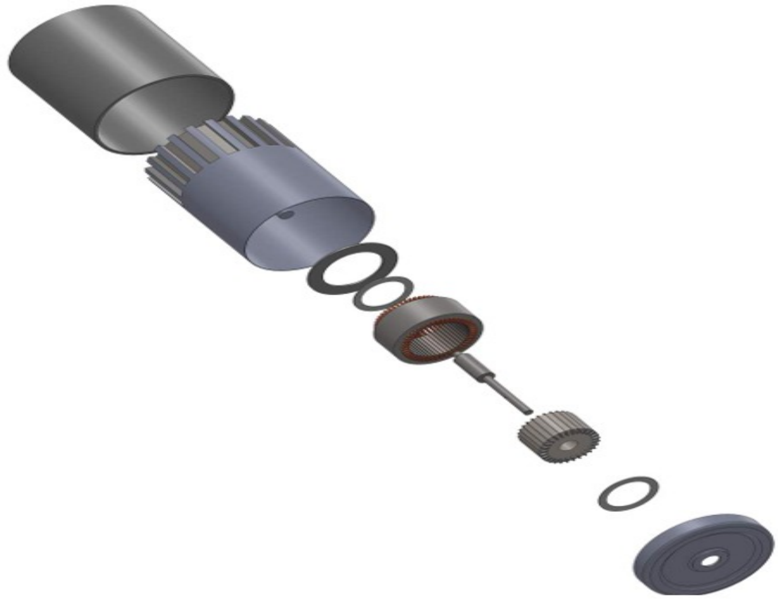

Fig. 1. Visualization of generator components

2.3 Material Models and Thermal Properties

The selection of materials in the simulation aims to accurately replicate the heat transfer behavior occurring in offshore wind turbine generators. The focus of this study is the application of *Phase Change Materials* (PCM) as latent heat storage media to enhance cooling performance. Three PCM types—paraffin, salt hydrate, and eutectic mixtures—were examined due to their distinct thermal characteristics. As summarized in Table 2, paraffin was selected for its stability, availability, and chemical inertness, while salt hydrates were chosen for their high latent heat capacity despite their susceptibility to supercooling. Eutectic mixtures were also considered because their melting points can be precisely adjusted to match the operational temperature range of the generator, ensuring efficient thermal regulation [15,16].

Each PCM type exhibits unique thermal properties that influence its heat transfer behavior. The main parameters considered in the simulation include density, latent heat of fusion, specific heat capacity, and thermal conductivity, which determine the PCM's heat absorption and release performance. The generator's structural materials—copper, steel, and epoxy-based insulation—were also modeled based on their standard thermal properties, as detailed in Table 3. These material definitions ensure realistic representation of the conduction and convection mechanisms within the generator housing. The latent heat behavior of the PCM, which plays a critical role in delaying temperature rise during operation, is illustrated in Figure 2, highlighting the phase transition process from solid to liquid. With accurate material data derived from experimental literature, the CFD simulation can effectively reproduce the real heat transfer conditions of offshore wind turbine generators [17].

Table 2
Thermal properties of PCM material [9,10,18]

Types of PCM	Melting Point (°C)	Latent Heat (kJ/kg)	Thermal Conductivity (W/m·(K)	Specific Heat Capacity (kJ/kg·(K)	Density (kg/m3)
Paraffin	48 – 60	150 – 200	0,2 – 0,3	2,0 – 2,5	770 - 900
Hydrated Salt	28 – 50	200 – 300	0,5 – 0,7	1,5 – 2,0	1400 – 1600
Euthetic mixtures	20 - 40	180 - 250	0,3 – 0,5	1,8 – 2,2	1100 - 1300

Table 3
Thermal properties of generator constituent materials [7,19,20]

Metarial	Thermal Conductivity (W/m-K)	Specific Heat Capacity (kJ/kg-K)	Density (kg/m3)
Copper	385 – 400	0,38 – 0,39	8900
Steel	45 – 55	0,46 – 0,50	7850
Isolator (epoxy, resin)	0,2 – 0,3	1,0 – 1,3	1100 – 1400

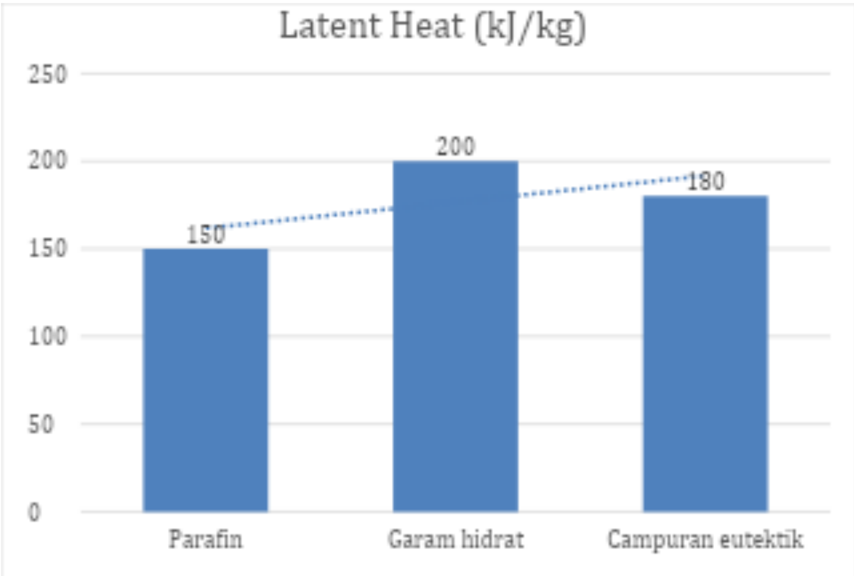

Fig. 2. Heat latent PCM material

2.4 Mathematical Formulation and PCM Model

The heat transfer phenomenon in the cooling system of offshore wind turbine generators with PCM integration is analyzed using the CFD numerical approach [21]. The applied mathematical formulation refers to the basic laws of conservation of mass, momentum, and energy, and is solved numerically on a simplified domain of geometry.
Continuity Equation

$$\nabla . \vec{v} \quad (1)$$

The Momentum Equation (Navier-Stokes Equation)

$$\rho \left(\frac{\partial \vec{v}}{\partial t} + \vec{v}. \nabla \vec{v} \right) = -\nabla p + \mu \nabla^2 \vec{v} + \vec{F} \quad (2)$$

Energy Equation

$$\rho c_p \frac{\partial T}{\partial t} + \rho c_p \vec{v}.\nabla T = \nabla.(k\nabla T) + S_T \quad (3)$$

Thermal sources in the energy equation

$$H = h + \Delta H = \int_{T_{ref}}^{T} C_p dT + \beta L \quad (4)$$

Simulation assumptions and conditions

The airflow is considered turbulent and modeled using the *k–ε* turbulence model to simulate forced convection around the generator housing. Simulations were conducted under transient conditions to ensure accurate prediction of PCM melting and solidification behavior. The heat transfer interface between the stator, housing, and PCM unit was defined through a conduction–convection boundary condition, while the stator heat source was introduced as a heat generation rate. This CFD framework captures the complex interactions between cooling airflow, solid material conduction, and latent heat storage within the PCM. The overall numerical workflow—including meshing, model setup, numerical solution, and post-processing procedures—is illustrated in Figure 3, which outlines the computational process used to evaluate temperature distribution, PCM liquid fraction, and peak temperature reduction for various PCM configurations [2].

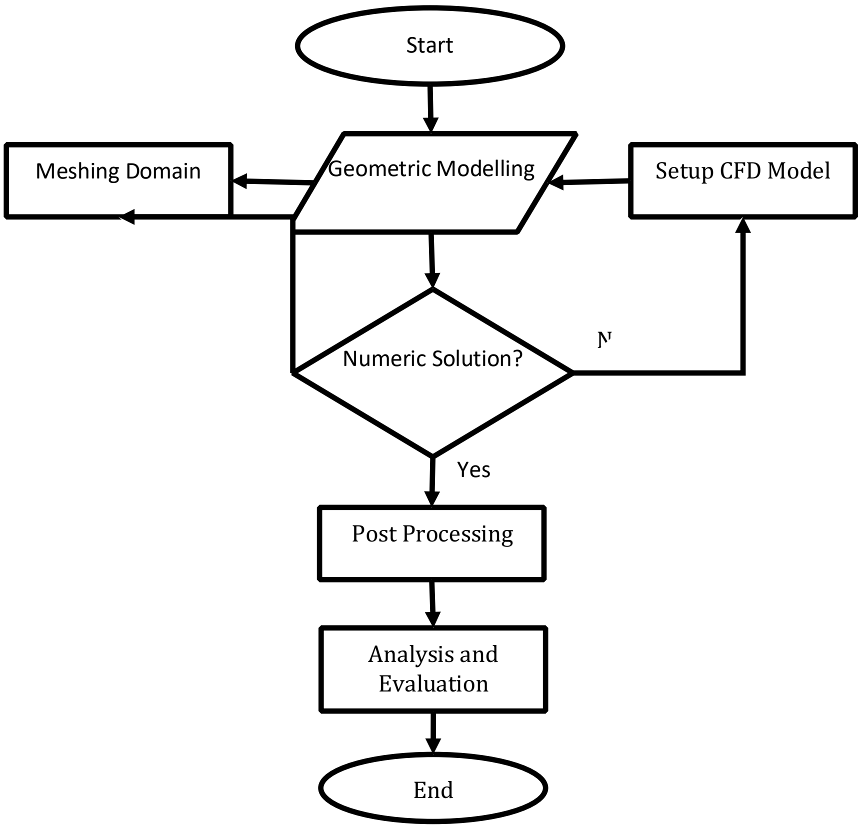

Fig 3. Flowchart procces

Computational Fluid Dynamics (CFD) simulation is designed as a systematic procedure to solve continuous flow problems governed by the conservation equations of mass, momentum, and energy. The process begins with defining the physical objectives and boundary conditions of the problem, followed by geometric modeling and discretization of the domain using suitable meshing techniques to ensure numerical consistency. The next step involves selecting the physical and numerical models, including turbulence models, material properties, and boundary as well as initial conditions, accompanied by appropriate temporal and spatial discretization schemes such as the finite volume, finite element, or finite difference methods. Solver iterations are then executed using linearization, residual balancing, and relaxation strategies until the convergence criteria are satisfied, supported by numerical verification and validation when reference data are available. After achieving convergence, quantitative and visual post-processing is performed for the extraction of derived parameters, sensitivity analysis, and identification of critical thermal phenomena. The overall simulation workflow is summarized in Table 4, which presents the detailed CFD simulation parameters including mesh type, boundary conditions, solver setup, and output variables used to analyze generator temperature distribution, PCM liquid fraction, and heat absorption efficiency [23], [24].

Table 4
CFD simulation parameters summary

Category	Parameters	Grades/Description
Meshing	Simulation domains	Simple generator + capping PCM unit
	PCM Location	Around stator winding & housing (hot-spot area)
	Mesh type	Hybrid (tetrahedral + hexahedral in critical areas)
	Minimum element size	1 – 2 mm around stator and PCM
	Maximum element size	5 – 10 mm in the fluid area
	Schema refinement	Local mesh refinement on PCM–solid interface
Physical Model	Flow model	Turbulent, k–ε standard
	Heat transfer	Conduction + convection + phase-transition PCM
	Model PCM	Enthalpy–Porosity method
Boundary Conditions	Heat generation rate (stator)	5–15 kW (load scenario variation)
	Inlet air temperature	25°C (assumption of offshore marine environment)
	Boundary housing	Natural convection/forced convation. (h = 10–30 W/m²· K)
Solver	Types of analysis	Transient (time-dependent)
	Time step	0.1 – 1 sec (Adaptive)
	Total duration of the simulation	600 – 1200 s (10–20 minutes real-time)
	Convergence criteria	10^{-5} for energy, 10^{-4} for mass & momentum
Main Output	Generator temperature distribution	[°C]
	PCM liquid fraction	0 – 1
	Heat absorption efficiency	% PCM absorbed peak load energy
	Drop in peak temperatures	Maximum ΔT [°C]

2.5 Boundary Conditions and Simulation Scenarios

In this study, the boundary conditions reflect the actual operation of offshore wind turbine generators. The heat load of the generator is determined at 50%, 75%, and 100% full capacity. It aims to assess the performance of the cooling system from partial condition to maximum load, where heat dissipation increases due to the electric current in the winding stator. In this way, the thermal characteristics of the generator are observed at different levels of thermal stress. Environmental conditions are adapted to the offshore marine climate which has an ambient temperature between 25–35 °C. The heat transfer on the surface of the generator casing is modeled through natural and forced convection. The convection coefficient is determined from the literature, which is 10–30 $W/m^2 \cdot K$ for natural convection and 50–100 $W/m^2 \cdot K$ for forced convection due to air flow from sea breezes. The cooling design scenario tested includes five main configurations. First, a conventional cooling system without PCM as a reference. Second, the cooling system with paraffin-based PCM which has good chemical stability. Third, a cooling system with a PCM based on salt hydrate that offers high latent heat but has the challenge of cycle stability. Fourth, a cooling system with PCM based on eutectic mixtures to obtain the optimal melting point according to the generator's operating range. Fifth, variation of the position of the PCM capsulation on the critical heat path around the winding stator and housing to determine an effective placement configuration in reducing temperature fluctuations [25].

2.6 Simulation Procedure

The simulation process uses CFD software such as Ansys workbench Multiphysics to solve the heat transfer equation numerically. The procedure is structured from pre-processing to analysis of simulated results for consistency. The first stage is pre-processing, including the creation of geometric models and PCM units, meshing the simulation domain, as well as determining the properties of the material. The geometry is simplified to maintain the accuracy of the calculations. Meshing uses tetrahedral and hexahedral elements with finer sizes in critical areas such as stator winding and PCM–housing interfaces. The properties of the materials included include thermal conductivity, specific heat capacity, density, and PCM latent heat from the literature.

The second stage is the solver setup, which sets up the physical and numerical conditions for the simulation. Physical models include k-ε turbulence, conduction-convection heat transfer, and PCM modeling using enthalpy-porosity methods for phase transitions. The numerical scheme uses the second-order upwind method for solution stability, with simulations running in transient conditions and a time step of 0.1–1 seconds as required. Boundary conditions are set according to the simulation scenario, including variations in heat load, ambient temperature, and convection coefficient on the housing surface [26].Until the system is stable, the third step is simulation, which involves numerical computations. The process is repeated while keeping an eye on the residual until the convergence criteria—10^{-5} for energy and 10^{-4} for mass and momentum—are met. To prevent numerical instability, variables including stator temperature, PCM liquid fraction, and heat flux are tracked during this procedure. The last stage is post-processing, which analyzes the results of the simulation. Data include temperature distribution in domains, peak temperature reduction in statators, and critical temperature achievement delay due to PCM. PCM visualization of temperature and liquid fraction graphs is used to evaluate the effectiveness of the cooling design. Comparison of various simulation scenarios assesses the performance of PCMs based on material type, capsulation geometry, and integration position [27].

2.7 Evaluation Parameters

A series of assessment metrics were established based on relevant thermal performance indicators to evaluate the effectiveness of the cooling system in offshore wind turbine generators integrated with *Phase Change Materials* (PCM). These indicators form the basis for comparing PCM-based cooling configurations with conventional systems, considering both the type of PCM and its integration position. The first evaluation parameter is the maximum generator temperature (°C), which represents the highest temperature at the stator winding or housing. A lower peak temperature indicates a more effective cooling system in mitigating overheating, thereby extending generator lifespan, minimizing material degradation, and maintaining insulation reliability.

The second parameter is the delay time in reaching the critical temperature. PCMs with high latent heat capacity can absorb excess thermal energy, thus delaying the temperature rise toward unsafe operational limits. The third parameter concerns temperature distribution and thermal homogeneity, which reflect the system's ability to prevent localized hot spots that could damage structural or electrical components. The fourth parameter evaluates the latent heat storage efficiency of the PCM, defined as the percentage of total heat energy stored in the form of phase change. Finally, the fifth parameter is thermal cycle stability under repeated load fluctuations, which assesses the PCM's ability to maintain its thermal characteristics during successive melting–solidification cycles caused by variable wind speeds. All five parameters are summarized in Table 5, which outlines the measurement units and objectives of each thermal performance indicator used in the study. These evaluation metrics provide a comprehensive framework for analyzing the cooling performance, heat storage effectiveness, and long-term reliability of PCM-integrated generator systems [28].

Table 5
Evaluation parameters of generator cooling system with PCM

Parameters	Unit	Measurement Objectives
Maximum temperature of the generator	°C	Assess the peak temperature of the stator/housing and the effectiveness of cooling in preventing overheating.
Delay in reaching critical temperature	S	Measuring the PCM's ability delays temperature rise until it has passed the critical operating limit.
Temperature distribution and heat homogeneity	°C / CFD Contour	Evaluate the temperature spread within the generator to detect potential *hot spots*.
PCM latent heat storage efficiency	%	Determines the proportion of the heat energy that the PCM can absorb/store from the total energy released.
Thermal cycle stability under repeated loads	-(qualitative/quantitative)	Assess the ability of PCM to retain its thermal properties after repeatedly undergoing the thaw-freeze cycle.

2.8 Formula and Method of Calculating Evaluation Parameters

1. Maximum temperature of the generator [10].

$$T_{max}(t) = \ T(x,t) \quad (5)$$

2. Delay in reaching critical temperature

$$t_{delay}(t) = min\{t : T_{max}(t) \geq \ T_{crit}\} \quad (6)$$

3. Temperature distribution & heat homogeneity
   - Average temperature (mean):

$$\vec{T}(t) = \frac{1}{V}\int_V \quad T(x,t)dV \tag{7}$$

- Standard deviation (marker of homogeneity):

$$\sigma_t(t) = \sqrt{\frac{1}{V}\int_V \quad \left(T(x,t) - \vec{T}\right)^2 dV} \tag{8}$$

- Coefficient of variation (CV):(normalization)

$$CV(t) = \frac{\sigma_T(t)}{\underline{T}(t)} \tag{9}$$

- Nominal homogeneity index (optional):

$$H(t) = 1 - \frac{\sigma_T(t)}{T_{max}(t) - T_{min}(t)} \tag{10}$$

- CFD implementation (discrete): if the discrete domain with volume cells *Vi* and *Ti*

$$\underline{T} \approx \frac{\sum_i \quad T_i V_i}{\sum_i \quad T_i V_i}, \sigma_T \approx \sqrt{\frac{\sum_i \quad (T_i - \underline{T})^2 V_i}{\sum_i \quad V_i}}$$

(11)

4. PCM latent heat storage efficiency

- Total energy released by the generator (in time intervals of $0 = t$) [29]:

$$Q_{gen}(0 \to t) = \int_0^t \quad \dot{Q}_{gen}(t')dt' \tag{12}$$

- Energy stored by PCM (sensitive + latent energy) [30]:

$$Q_{PCM}(0 \to t) = \int_{V_{PCM}} \quad \rho\left[h\left(T(x,t)\right) - h\left(T(x,0)\right)\right]dV \tag{13}$$

- Storage efficiency (percent):

$$\eta_{PCM}(t) = 100\% \times \frac{Q_{PCM}(0 \to t)}{Q_{gen}(0 \to t)} \tag{14}$$

- Practical enthalpy calculation (entalpy–porosity model): if cp is considered constant:

$$h(T) \approx C_p\left(T - T_{ref}\right) + \beta(T)L \tag{15}$$

- CFD implementation (discrete): for i cells in *VPCM* [31]*:*

$$Q_{PCM} \approx \sum_i \quad \rho i[C_{p,i}(T_i - T_{i,0}) + \beta_i L_i]V_i \tag{16}$$

5. Thermal cycle stability under repeated loads
   - Latent heat retention capability: measure the change in effective latent capacity after *N* cycle:
     $$\Delta L_{\%}(N) = 100\% \times \frac{L(N)-L(0)}{L(0)} \tag{17}$$
   - Another method of loss of performance per cycle: compare tdelay or Tmax on the 1st cycle and the *N cycle*.
     $$degradasi_t = \frac{t_{delay}(N)-t_{delay}(1)}{t_{delay}(1)} \times 100\% \tag{18}$$
   - Monitoring the average liquid fraction per cycle:
     $$\underline{\beta}_{cycle} = \frac{1}{t_{cycle}} \int_0^{t_{cycle}} \quad (\frac{1}{V_{PCM}} \int_{V_{PCM}} \quad \beta(x,t)dV)d \tag{19}$$

3. Results

The following results section presents a detailed discussion for each configuration tested—without PCM (baseline), with paraffin PCM, hydrate salt PCM, and eutectic mixed PCM—and links each quantitative finding to the relevant simulation visualization at Figure 4-6. For each configuration are systematically discussed: temperature distribution within the domain, peak temperature drop at full load, temperature homogeneity and coefficient of variation, evolution of liquid fraction and delay time to reach critical thresholds, latent heat storage efficiency and cycle stability, and influence of capsulation and placement geometry on thermal performance; Each point is directly referenced to a supporting image or graph so that the reader can verify the numerical claim from the available visualization.

3.1 Thermal Characterization of the Reference without PCM

Around the circumference of the stator with very dense isotherms so that a centralized hotspot is formed, while Figure 4 emphasizes the radial profile which shows a sharp drop in temperature from the stator core to the casing due to thermal resistance in the internal conduction–convection pathway; quantitatively in this conditional full load scenario it produces a peak temperature of TMax ≈ 105 °C and a volumetric average of ≈ 65 °C with a large standard deviation (σT ≈ 22.75 °C)

$$CV = \frac{\sigma_T}{T} = \frac{22{,}75}{65} \approx 0{,}35 \tag{20}$$

so that the CV coefficient of variation ≈ 0.35, a high indicator of thermal inhomogeneity; Without a latent storage mechanism, the thermal response is fast so that the delay time towards the critical threshold (e.g. Tcrit = 95°C) is relatively short, increasing the frequency of thermal cycles and the risk of insulation degradation; Spatial analysis also showed that local thermal resistance was likely due to a combination of low conductivity of insulating materials, limited thermal contact between windings and metal structures, and geometry that restricted airflow paths, so design recommendations include increasing the conductivity of internal pathways (e.g., thermal fillers or thermal conductor pathways), expanding the heat exchange area between the windings and housings, and consideration of placement of thermal storage elements or improvements forced convection effect to flatten the temperature map, lower the TMax, reduce σT and CV, and extend the delay to improve operational reliability.

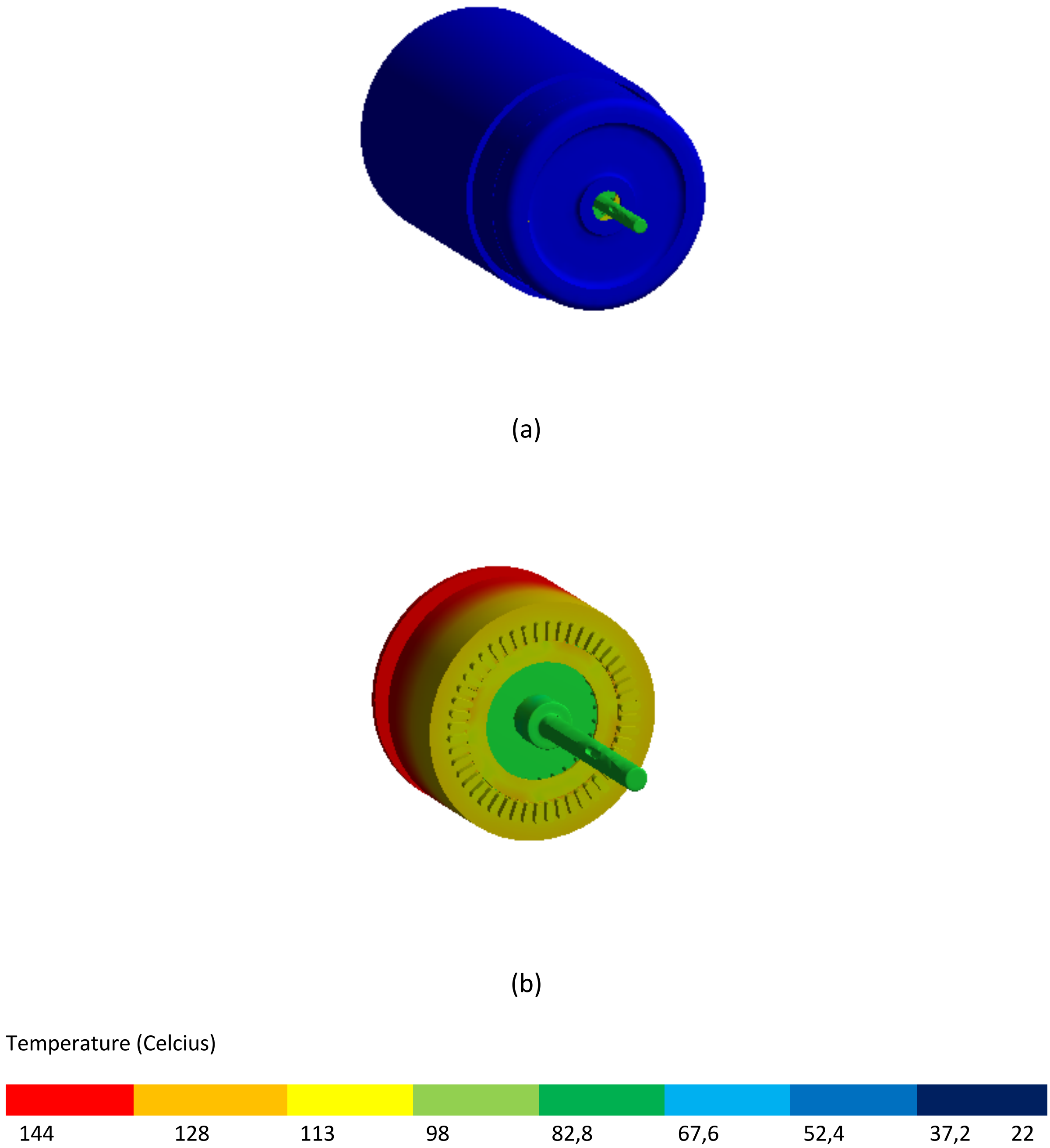

Fig. 4. Ilustrasion contour of (a) Temperature housing of generator without PCM, (b) Rotor and stator isometric without PCM

3.2 Impact of PCM Paraffin Integration

The application of PCM paraffin (melting point 48–60 °C, latent heat 150–200 kJ/kg) resulted in a significant but moderate decrease in peak temperature compared to baseline. The temperature contour in Figure 5a and the crosssection in Figure 5c show the thermal buffer zone around the stator winding; Tmax decreases by about 18–20% relative to baseline (see numerical comparison in Figure 5b [32]. The integration of paraffin forms a thermal buffer layer around the stator so that the heat isothermal shifts from red to orange and the hotspot shrinks locally Figure 5a, resulting in a Tmax decrease of about 18–20% quantified in the comparison diagram Figure 5a. This effect increases the homogeneity of the temperature: the CV drops from ~0.35 to ~0.20–0.22 Figure 5c. but the rate of liquefaction is relatively slow so that the extension of the tdelay time is only moderate—the fluid fraction progression and the Tmax vs time curve are in Figure 5c. Practically paraffin offers a clear tradeoff: good cyclic stability and latent energy retention are adequate for long-term operation, but require high surface area capsulation or the addition of conductive fillers to improve the transient response to load spikes.

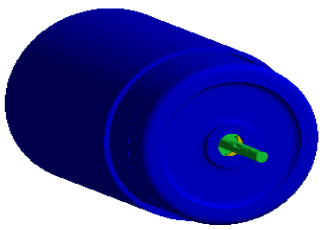

(a)

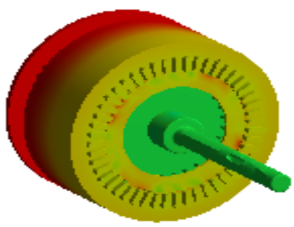

(b)

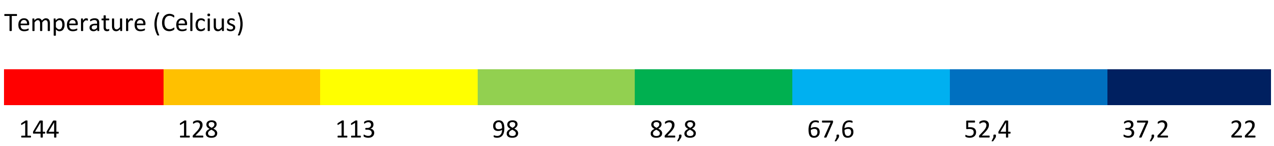

Fig. 5. Ilustrasion contour of (a) Temperature housing of generator with PCM paraffin wax, (b) Rotor and stator isometric with PCM paraffin wax

3.3 Impact of PCM Integration of Hydrate Salts

The integration of hydrate salts consistently results in the most significant thermal improvements compared to other configurations; the temperature contour in Figure 6a and the radial cross-section in Figure 6c show a reduction in hotspot volume around the stator circumference as the isotherm is pushed towards the PCM unit, making the local heat dissipation path more effective. At full load measurements show a peak temperature decrease of about 22–25% against baseline, the values summarized in the comparison, while the coefficient of temperature variation drops to the lowest range (~0.18) which indicates the best thermal homogeneity among all cases.

The transient dynamics of the hydrate salts are also superior: the liquid fraction increases rapidly so that the longest period of delay of reaching the critical temperature (tdelay) is reached, which is clearly seen in the Tmax vs time panel in Figure 6c with the shading of the tdelay period. The latent storage efficiency is relatively high due to the combination of latent heat and large density, but the practical aspect demands mitigation against the risk of supercooling and thermal degradation; The cyclic degradation trend can be monitored at the stability inset. By design, capsulation optimization—e.g., microencapsulation with conductive fillers or structured packedbeds as in the schematic Figure 6c —is necessary to maximize surface transfer, control cyclic phenomena, and ensure long-term performance.

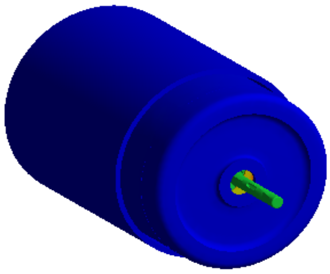

(a)

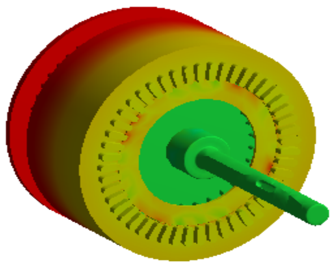

(b)

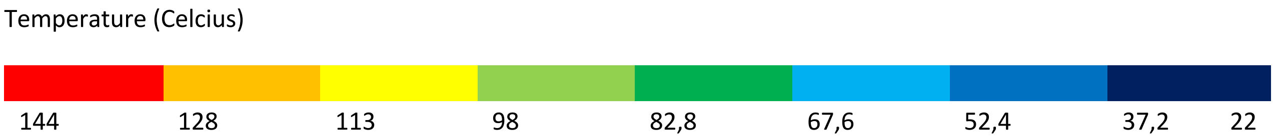

Fig. 6. Ilustrasion contour of (a) Temperature housing of generator with PCM hydrate salts, (b) Rotor and stator isometric with PCM hydrate salts

3.4 Impact of Eutectic Mixed PCM Integration

The temperature contour for the eutectic mixture configuration shows a clear isothermal leveling in the transition zone between the stator and the housing, forming a thermal buffer layer that effectively inhibits hotspot formation Figure 7a. At full load, eutectic integration lowers the peak temperature by approximately 20–23%, while the coefficient of temperature variation narrows to the range of ~0.19–0.21, indicating a temperature homogenization that is close to the performance of hydrate salts without an increased risk of degradation equivalent to hydrate salts. The dynamics of eutectic liquefaction are between paraffin and salt hydrate so that the liquid fraction increases at a moderate rate and extends the delay time towards the critical threshold at the simulation duration (see the evolution of the liquid fraction and the Tmax curve in Figure 7b. By design, capsulation structures such as thin packedbeds or medium-conductivity PCM layers provide the best tradeoff between transient response and latent capacity; this option optimizes Tmax drop and heat homogeneity while maintaining relatively better cyclic stability, as shown in the performance comparison visualization in Figure 7a-c.

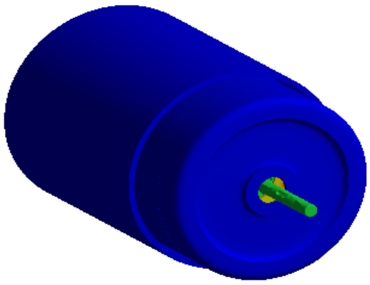

(a)

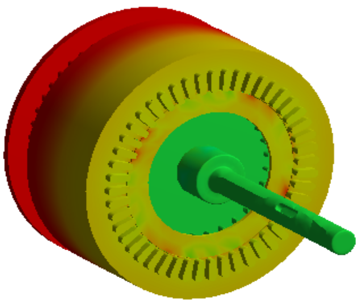

(b)

Temperature (Celcius)

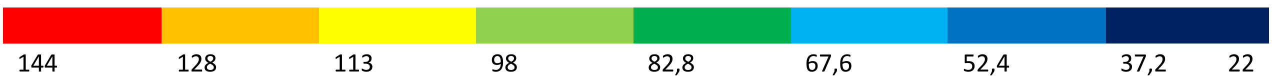

Fig. 7. Ilustrasion contour of (a) Temperature housing of generator with eutectic mixed PCM integration, (b) Rotor and stator isometric with eutectic mixed PCM integration

4. Conclusions

The results of the CFD study show that the integration of PCM into the cooling system of offshore wind turbine generators consistently improves thermal efficiency compared to conventional configurations: the use of PCM lowers peak temperatures by about 15–25% and extends the delay time to reach critical thresholds thereby reducing the frequency of thermal cycles; among the tested materials hydrated salts provided the greatest thermal improvement (~22–25% Tmax decrease and best homogeneity), eutectic mixtures provided intermediate performance with a balance of transient response and latent capacity (~20–23% decrease in Tmax), while paraffin produced moderate decline (~18–20%) with the highest cyclic stability but relatively slow dilution response; the final effectiveness is strongly influenced by the latent heat capacity, melting point adjusted to operating conditions, thermal conductivity of the PCM–component interface, capsulation geometry, and placement location around the stator/housing winding; for practical implementation, it is recommended to optimize the selection of PCM (taking into account the risk of supercooling and cyclic degradation), increased heat transfer through capsulation and conductive fillers or structured packed beds, strategic placement on critical heat paths, as well as long-term cyclic testing and experimental validation to ensure long-term performance and reliability.

References

[1] Laghari, Imtiaz Ali, A. K. Pandey, M. Samykano, Reji Kumar Rajamony, Yasir Ali Bhutto, Abdul Hameed Soomro, K. Kadirgama, and V. V. Tyagi. "Binary nano-enhanced phase change materials (BNePCMs) integrated serpentine flow based photovoltaic thermal system: A new approach towards performance enhancement." *Thermal Science and Engineering Progress* 53 (2024): 102704. https://doi.org/10.1016/j.tsep.2024.102704

[2] Ali, Mohamed, Ahmed K. Alkaabi, and Jeong Ik Lee. "CFD simulation of an integrated PCM-based thermal energy storage within a nuclear power plant connected to a grid with constant or variable power demand." *Nuclear Engineering and Design* 394 (2022): 111819. https://doi.org/10.1016/j.nucengdes.2022.111819

[3] Arifin, Zainal, Bhimo Ageng Tribhuwana, Budi Kristiawan, D. D. D. P. Tjahjana, Syamsul Hadi, Rendy Adhi Rachmanto, Singgih Dwi Prasetyo, and Miftah Hijriawan. "The effect of soybean wax as a phase change material on the cooling performance of photovoltaic solar panel." *International Journal of Heat and Technology* 40, no. 1 (2022): 326-332. https://doi.org/10.18280/ijht.400139

[4] Basem, Ali, Ammar M. Al-Tajer, Ihab Omar, Hayder A. Dhahad, and Wissam H. Alawee. "Improvement of heat transfer within phase change materials using V-shaped rods." *Heliyon* 10, no. 7 (2024). https://doi.org/10.1016/j.heliyon.2024.e28146

[5] Bianco, Vincenzo, Mattia De Rosa, and Kambiz Vafai. "Phase-change materials for thermal management of electronic devices." *Applied Thermal Engineering* 214 (2022): 118839. https://doi.org/10.1016/j.applthermaleng.2022.118839

[6] Durez, Asif, Muzaffar Ali, Adeel Waqas, Kamran Nazir, and Sudhakar Kumarasamy. "Modelling and optimization of phase change materials (PCM)-based passive cooling of solar PV panels in multi climate conditions." *Frontiers in Energy Research* 11 (2023): 1121138. https://doi.org/10.3389/fenrg.2023.1121138

[7] Prasetyo, Singgih Dwi, Yuki Trisnoaji, Zainal Arifin, and Abram Anggit Mahadi. "Harnessing unconventional resources for large-scale green hydrogen production: An economic and technological analysis in Indonesia." *Unconventional Resources* 6 (2025): 100174. https://doi.org/10.1016/j.uncres.2025.100174

[8] Grün, Thorsten, Kevin Stella, and Olaf Wollersheim. "Influence of circuit design on load distribution and performance of parallel-connected Lithium ion cells for photovoltaic home storage systems." *Journal of Energy Storage* 17 (2018): 367-382. https://doi.org/10.1016/j.est.2018.03.010

[9] Ibrahim, Tarek, Modar El Hazar, Farouk Hachem, and Mahmoud Khaled. "A comprehensive experimental study of cooling photovoltaic panels using phase change materials under free and forced convection–Experiments and transient analysis." *Journal of Energy Storage* 81 (2024): 110511. https://doi.org/10.1016/j.est.2024.110511

[10] Khalil, Essam E., and Mohamed Sobhi. "CFD simulation of thermal and energy performance for a display cabinet refrigerator containing a phase change material (PCM)." In *AIAA Propulsion and Energy 2020 Forum*, p. 3946. 2020. https://doi.org/10.2514/6.2020-3946

[11] Kibria, Md Golam, Utpol K. Paul, Md Shahriar Mohtasim, Barun K. Das, and N. N. Mustafi. "Characterization, optimization, and performance evaluation of PCM with Al2O3 and ZnO hybrid nanoparticles for photovoltaic

thermal energy storage." *Energy and Built Environment* (2024). https://doi.org/10.1016/j.enbenv.2024.06.001

[12] Kim, Soonwook, Tianyu Yang, Nenad Miljkovic, and William P. King. "Phase change material integrated cooling for transient thermal management of electronic devices." *International Journal of Heat and Mass Transfer* 213 (2023): 124263. https://doi.org/10.1016/j.ijheatmasstransfer.2023.124263

[13] Martínez, Arnold, Mauricio Carmona, Cristóbal Cortés, and Inmaculada Arauzo. "Experimentally based testing of the enthalpy-porosity method for the numerical simulation of phase change of paraffin-type PCMs." *Journal of Energy Storage* 69 (2023): 107876. https://doi.org/10.1016/j.est.2023.107876

[14] Mauludin, Mochamad Subchan, Moh Khairudin, Rustam Asnawi, Yuki Trisnoaji, Singgih Dwi Prasetyo, Safira Rusyda Azizah, and Rayie Tariaranie Wiraguna. "Assessing the Technological and Financial Feasibility of PV-Wind Hybrid Systems for EV Charging Stations on Indonesian Toll Roads." *International Journal of Sustainable Development & Planning* 20, no. 1 (2025). https://doi.org/10.18280/ijsdp.200127

[15] Murali, G., J. Emeema, B. Venkateswara Reddi, P. S. N. Masthan Vali, P. V. Elumalai, M. Murugan, Mamdooh Alwetaishi, T. Bhargava Ramu, and S. Prabhakar. "Study of thermal performance and melting behaviour of a novel paraffin wax-carbon quantum Dots PCMs." *Scientific reports* 15, no. 1 (2025): 30066. https://doi.org/10.1038/s41598-025-08312-8

[16] Nabwey, Hossam A., and Maha A. Tony. "Enhancing the performance of paraffin's phase change material through a hybrid scheme utilizing sand core matrix." *Scientific Reports* 14, no. 1 (2024): 20755. https://doi.org/10.1038/s41598-024-71848-8

[17] Prasetyo, Singgih Dwi. "Enhancing Thermal Efficiency of Lithium-Ion Batteries Using Phase Change Materials: A CFD-Based Comparative Study." *Journal of Research in Nanoscience and Nanotechnology* 17, no. 1 (2025): 7-23.

[18] Polikarpova, Maria, Pavel Ponomarev, Pekka Röyttä, Scott Semken, Yulia Alexandrova, and Juha Pyrhönen. "Direct liquid cooling for an outer-rotor direct-drive permanent-magnet synchronous generator for wind farm applications." *IET Electric Power Applications* 9, no. 8 (2015): 523-532. https://doi.org/10.1049/iet-epa.2014.0342

[19] Prasetyo, Singgih Dwi, Zainal Arifin, Aditya Rio Prabowo, and Eko Prasetya Budiana. "The Impact of Cavity in Finned Thermal Collector on PVT Performance Using Al2O3 Nanofluid." *International Journal of Thermofluids* (2025): 101284. https://doi.org/10.1016/j.ijft.2025.101284

[20] Prasetyo, Singgih Dwi, Aditya Rio Prabowo, and Zainal Arifin. "Investigation of Thermal Collector Nanofluids to Increase the Efficiency of Photovoltaic Solar Cells." *International Journal of Heat & Technology* 40, no. 2 (2022). https://doi.org/10.18280/ijht.400208

[21] Selvan, Jayakumar, and Sreekanth Manavalla. "Numerical analysis of E-machine cooling using phase change material." *Energies* 15, no. 15 (2022): 5594. https://doi.org/10.3390/en15155594

[22] Senga, Mariko, and Shinya Hasegawa. "Four-stage loop-type cascade traveling-wave thermoacoustic engine." *Applied Thermal Engineering* 104 (2016): 258-262. https://doi.org/10.1016/j.applthermaleng.2016.05.013

[23] Shaeli, Mays N., Jalal M. Jalil, and Mounir Baccar. "Improving the performance of solar photovoltaic thermal cells using jet impingement and phase change materials cooling technology." *Renewable Energy* 227 (2024): 120536. https://doi.org/10.1016/j.renene.2024.120536

[24] Sun, Hao, Yingjie Li, Zhiguo Bian, Xianyao Yan, Zeyan Wang, and Wenqiang Liu. "Thermochemical energy storage performances of Ca-based natural and waste materials under high pressure during CaO/CaCO3 cycles." *Energy Conversion and Management* 197 (2019): 111885. https://doi.org/10.1016/j.enconman.2019.111885

[25] Taras, Petrica, Reza Nilifard, Zi-Qiang Zhu, and Ziad Azar. "Cooling techniques in direct-drive generators for wind power application." *Energies* 15, no. 16 (2022): 5986. https://doi.org/10.3390/en15165986

[26] Theeb, Ali Hussein F., and Ihsan Y. Hussain. "Numerical simulation of thermal performance of heat sink augmented with phase change material PCM integrated with solid and aluminum metal foam fins." *Heat Transfer* 53, no. 7 (2024): 3799-3826. https://doi.org/10.1002/htj.23113

[27] Tiwari, Awaneendra Kumar, Kalyan Chatterjee, and Vinay Kumar Deolia. "Application of copper oxide nanofluid and phase change material on the performance of hybrid photovoltaic–thermal (PVT) system." *Processes* 11, no. 6 (2023): 1602. https://doi.org/10.3390/pr11061602

[28] Trisnoaji, Yuki, Singgih Dwi Prasetyo, Mochamad Choifin, Catur Harsito, and Abram Anggit Mahadi. "Enhancing Efficiency in Small-Scale Hydropower: A Comprehensive Review of Archimedes Screw Turbine Design Innovations." *Semarak Engineering Journal* 9, no. 1 (2025): 1-15.

[29] Trisnoaji, Yuki, Singgih Dwi Prasetyo, Catur Harsito, Abram Anggit, and Mochamad Subchan Mauludin. "Exploring Pressure Dynamics in Rough-Surfaced U-Bend Pipelines: A Comparative Study of Water and Nanofluid Composites Across Varying Mass Flow Rates." *Semarak International Journal of Nanotechnology* 3, no. 1 (2024): 1-21. https://doi.org/10.37934/sijn.3.1.121

[30] Trisnoaji, Y., S. D. Prasetyo, M. S. Mauludin, C. Harsito, and A. Anggit. "Computational fluid dynamics evaluation of nitrogen and hydrogen for enhanced air conditioning efficiency." *J. Ind. Intell* 2, no. 3 (2024): 144-159.

https://doi.org/10.56578/jii020302
[31] Xiao, Yao, Pingrui Huang, Gaosheng Wei, Liu Cui, Chao Xu, and Xiaoze Du. "State-of-the-art review on performance enhancement of photovoltaic/thermal system integrated with phase change materials." *Journal of Energy Storage* 56 (2022): 106073. https://doi.org/10.1016/j.est.2022.106073
[32] Zhu, Yanlong, Gerald Englmair, Haotian Huang, Janne Dragsted, Yuan Yuan, Jianhua Fan, and Simon Furbo. "Numerical investigations of a latent thermal energy storage for data center cooling." *Applied Thermal Engineering* 236 (2024): 121598. https://doi.org/10.1016/j.applthermaleng.2023.121598